Theor. Comput. Fluid Dyn.
DOI 10.1007/s00162-009-0171-0

ORIGINAL ARTICLE

Dmitry Kolomenskiy · Kai Schneider

Numerical simulations of falling leaves using a pseudo-spectral method with volume penalization

Received: 3 December 2008 / Accepted: 24 September 2009

Abstract The dynamics of falling leaves is studied by means of numerical simulations. The two-dimensional incompressible Navier–Stokes equations, coupled with the equations governing solid body dynamics, are solved using a Fourier pseudo-spectral method with volume penalization to impose no-slip boundary conditions. Comparison with other numerical methods is made. Simulations performed for different values of the Reynolds number show that its decrease stabilizes the free fall motion.

Keywords Fluid–solid interaction · Free fall · Volume penalization method

PACS 47.63.-b

1 Introduction

The dynamics of falling leaves, being most remarkable for its aesthetics, is at the same time a phenomenologically rich and practically important subject. Generally speaking, it may be regarded as an example of a dynamical system exhibiting both regular and apparently chaotic behavior.

Scientific interest in this phenomenon dates back to the nineteenth century—Maxwell's paper is the earliest reference (see [8]). Kelvin, Tait and Kirchhoff considered motion of a solid body in an inviscid fluid. This Hamiltonian system has been studied since then by different authors (see, e.g., [4]). The free fall of thin plates in real fluids, more difficult for rigorous analysis, has been considered in experiments and in numerical simulations (see [9,1,2] and references therein).

An important manifestation of viscous effects are the cusp-like turning points of the trajectory, where the centre of mass of the plate elevates [1]. This motion may be regarded as 'passive' flight for its similarity with flapping of insect wings.

The dynamics of a falling plate is characterized by three dimensionless numbers: the Reynolds number Re, the dimensionless moment of inertia I^*, and, in a particular case of elliptical cross-section, its eccentricity e [1]. The Reynolds number is of special interest, since it gives an idea about the range of scales where winged animals can take advantage of the centre of mass elevation to facilitate flapping of their wings.

In this paper we study the influence of the Reynolds number in the range from 10 to 1100. We apply the fluid-structure interaction model reported in [11,10,7] to perform numerical simulations of falling leaves,

Communicated by H. Aref

D. Kolomenskiy(✉)
M2P2-CNRS, Universités d'Aix-Marseille, 38 rue Joliot-Curie, 13451, Marseille Cedex 20, France
E-mail: dkolom@L3m.univ-mrs.fr

K. Schneider
M2P2-CNRS and CMI, Universités d'Aix-Marseille, 39 rue Joliot-Curie, 13453, Marseille Cedex 13, France
E-mail: kschneid@cmi.univ-mrs.fr

Published online: 31 October 2009

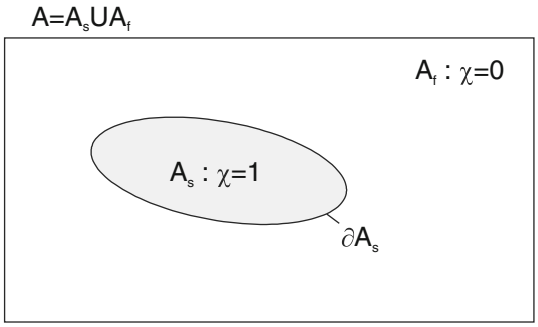

Fig. 1 The physical domain A containing the fluid domain A_f and the solid obstacle A_s with its boundary ∂A_s.

and show a stabilizing effect of decreasing Re. This result agrees with experimental observations made by Willmarth et al. [13] for falling circular disks, and then by Smith [12] for wings.

2 Physical model and numerical method

We consider interaction between viscous incompressible fluid and a solid body moving in it. The two-dimensional Navier–Stokes equations are written in the vorticity–stream function (ω-Ψ) formulation. Moving solid obstacles of arbitrary shape are taken into account using the volume penalization method. The penalized equations

$$\partial_t \omega_\eta + \mathbf{u}_\eta \cdot \nabla \omega_\eta - \nu \nabla^2 \omega_\eta + \nabla \times \left(\frac{\chi}{\eta} (\mathbf{u}_\eta - \mathbf{u}_s) \right) = 0, \tag{1}$$

$$\nabla^2 \Psi = \omega_\eta, \qquad \mathbf{u}_\eta = \nabla^\perp \Psi + \mathbf{U}_\infty, \tag{2}$$

are solved in the domain $A = A_f \bigcup A_s$ containing both the fluid and the solid obstacle (see Fig. 1). The viscosity of the fluid is ν, η is the penalization parameter, χ is the mask function describing the shape of the solid, $\mathbf{u}_s$ is the velocity field of the solid, $\mathbf{U}_\infty$ is the free-stream velocity, $\omega_\eta = \nabla \times u_\eta$ is the vorticity, and $\nabla^\perp = (-\partial_y, \partial_x)$. The density of the fluid is normalized to unity, $\rho = 1$. The volume penalization method is motivated by an idea of modelling solid obstacles as porous media with vanishing permeability. When η in Eq. (1) is tending to zero, the penalized problem converges to the no-slip boundary problem [3]. The fluid and the solid are thus considered as one medium with permeability varying in space and in time. This allows to implement efficiently and in a relatively straightforward manner such features as arbitrary shape and number of obstacles.

The motion of the solid is governed by Newton's second law, which yields ODEs for the center of gravity position $\mathbf{x}_{cg}$ and for the angle of incidence θ_{cg}.

$$m_b \frac{\mathrm{d}^2 \mathbf{x}_{cg}}{\mathrm{d}t^2} = \int_A \frac{\chi}{\eta} (\mathbf{u}_\eta - \mathbf{u}_s) \mathrm{d}A + m_b \mathbf{g}, \tag{3}$$

$$J_b \frac{\mathrm{d}^2 \theta_{cg}}{\mathrm{d}t^2} = \int_A \frac{\chi}{\eta} (\mathbf{x} - \mathbf{x}_{cg}) \times (\mathbf{u}_\eta - \mathbf{u}_s) \mathrm{d}A, \tag{4}$$

where m_b and J_b are, respectively, the buoyancy corrected mass and moment of inertia of the solid body. The integrals, as well as the buoyancy correction, represent the action of fluid forces calculated using the penalized model. Note that the integration is performed over the volume of the domain, and not over the surface of the solid body. This is more convenient for numerical evaluation.

For the spatial discretization of (1)–(2) we use a classical Fourier pseudo-spectral method. The temporal integration schemes are an adaptive second order Adams-Bashforth [10] for (1), with exact integration of the Laplacian, and a first-order explicit scheme for (3)–(4). The motion of the obstacle is modelled with a shift of the mask function. For its translation we rotate the phase of its Fourier coefficients:

$$\chi(x,t) = \chi_0(x - \delta x) \quad \Leftrightarrow \quad \widehat{\chi}(k,t) = e^{-ik\delta x} \widehat{\chi}_0(k), \tag{5}$$

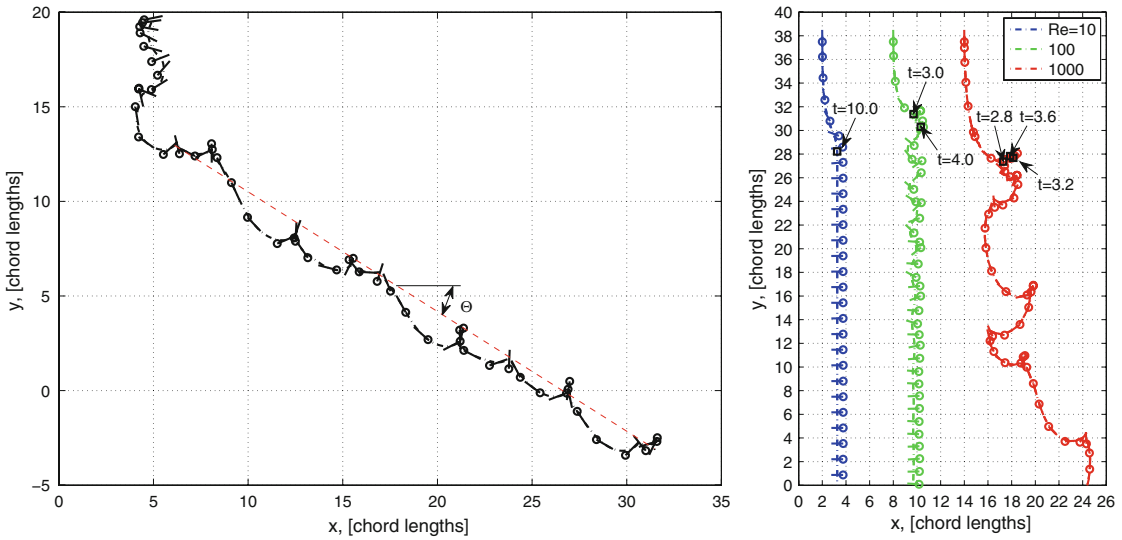

Fig. 2 *Left*: trajectory of the tumbling plate at $Re = 1100$. *Right*: trajectories of the plate dropped edge-on at three different Reynolds numbers (colour online).

Table 1 Averaged translational and angular velocities, and descent angle of the falling plate at $Re = 1100$

	U (cm/s)	V (cm/s)	Ω_z (1/s)	Θ (deg)
Present computation	11.3	−7.2	19.4	32.5
Andersen, Pesavento and Wang [1]	15.6	−7.4	18.0	25.3
Jin and Xu [6]	15.3	−11.2	16.9	36.2

where k is the wavenumber. Solid body rotation at an angle θ is decomposed into three skewing operations:

$$R(\theta) = \begin{bmatrix} \cos\theta & -\sin\theta \\ \sin\theta & \cos\theta \end{bmatrix} = \begin{bmatrix} 1 & -\tan(\theta/2) \\ 0 & 1 \end{bmatrix} \begin{bmatrix} 1 & 0 \\ \sin\theta & 1 \end{bmatrix} \begin{bmatrix} 1 & -\tan(\theta/2) \\ 0 & 1 \end{bmatrix}. \tag{6}$$

The mask function is smoothed in order to avoid Gibbs oscillations. This is done by applying a Gaussian filter to the discontinuous mask function. For further details on the numerical scheme we refer the reader to [7].

3 Results

As a matter of validation, we made a comparison with numerical results reported in [1] and [6]. A solid plate having an elliptical cross-section is considered for that purpose. Its eccentricity equals $e = b/a = 0.125$, and its dimensionless moment of inertia is $I^* = 0.5e(e^2 + 1)\rho_{solid}/\rho = 0.17$, where ρ_{solid} is the density of the solid. The Reynolds number is based on its size $2a$ and its terminal velocity, $u_t = \sqrt{\pi bg(\rho_{solid}/\rho - 1)}$, and it is equal to $Re = 1100$. The fluid is initially at rest. The plate is released from rest at an initial angle of incidence $\theta_0 = 0.2$. The periodic domain width and height are, respectively, $L_x = 10$ and $L_y = 20$ times the chord length of the plate. The domain is discretized with $N_x \times N_y = 1024 \times 2048$ grid points. The penalization parameter is $\eta = 10^{-3}$. Figure 2 (left) shows the trajectory of the tumbling plate, while a comparison of the average translational and angular velocities and the angle of descent with available values in [1,6] is presented in Table 1. The agreement between the three methods is rather reasonable, taking into account the sensitivity of the problem to perturbations, and the accuracy is satisfactory at least to make qualitative conclusions. More details on the validation of the numerical method can be found in [7].

To study the influence of viscosity on the dynamics of the plate, simulations at three different Reynolds numbers are performed: $Re = 10, 100$ and 1000. The plate, having the same elliptical cross-section as before, is released in a fluid at rest, with zero initial velocity and with its longer axis oriented almost vertically, $\theta_0 = \pi/2 + 0.01$ (a small deviation is needed to provoke instability). The periodic domain size equals $L_x \times L_y = 10 \times 40$ chord lengths, the number of grid points is $N_x \times N_y = 1024 \times 4096$, and $\eta = 10^{-3}$.

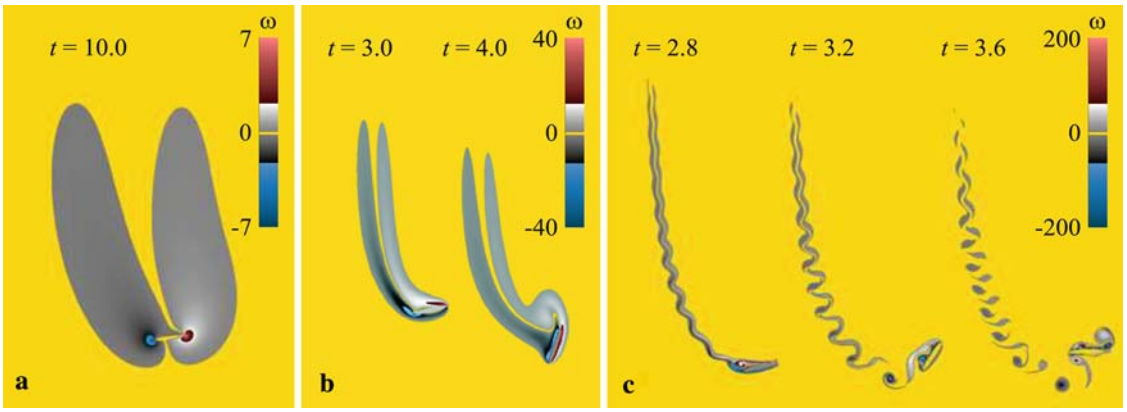

Fig. 3 Vorticity at $Re = 10$ (**a**), $Re = 100$ (**b**), and $Re = 1000$ (**c**) (colour online).

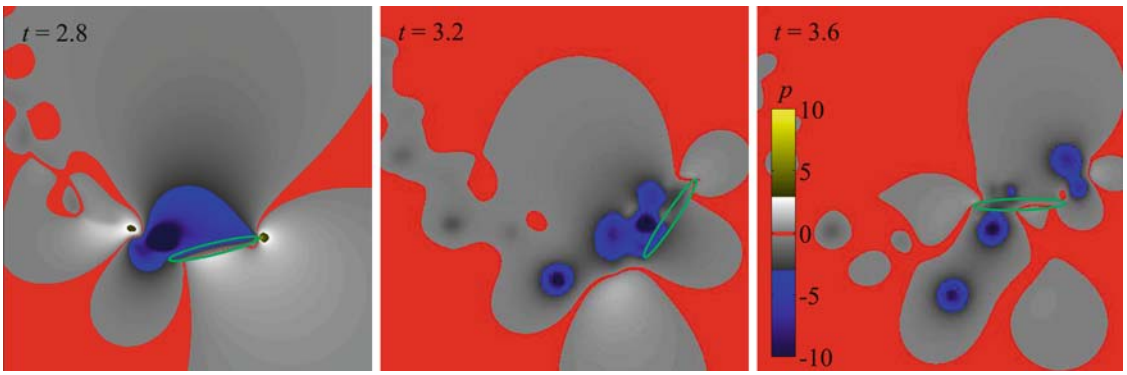

Fig. 4 Pressure field near the plate at $Re = 1000$, corresponding to Fig. 3c (colour online).

Figure 2 (right) shows three trajectories of the plate, corresponding to the three values of the Reynolds number. The vertical orientation is unstable in the range of Re concerned. At $Re = 10$ the plate falls broadside-on, after a short transient. At $Re = 100$ the same steady-state establishes, but the transient motion is oscillatory. A similar transient is reported in [13] for falling disks. At $Re = 1000$ the broadside-on state is no more stable, and the plate is moving in an apparently chaotic manner, rocking from side to side and occasionally overturning. This behaviour is consistent with the bifurcation diagram obtained experimentally in [12], where the point $Re = 1000$, $I^* = 0.17$ in parameter space lies on the border between the 'rocking motion range' and the 'autorotation range'. Note that $Re = 1000$ is just slightly lower with respect to the computation shown in the previous section, but, together with a different initial condition, this results in a qualitatively different behaviour: the plate did not reach a tumbling state.

Figure 3 displays corresponding vorticity snapshots for the same Reynolds numbers. The wake undergoes a transition between $Re = 100$ and $Re = 1000$. At higher Re it contains distinct vortical structures formed due to hydrodynamic instabilities. Interactions between the intensive vortices and the plate are complex (see an example in Fig. 3c), and extremely sensitive to perturbations. In contrast, at lower Re the wake is stable and the vorticity field is much smoother (see Fig. 3 a, b).

Figure 4 shows the pressure field near to the plate at $Re = 1000$ at consecutive time instants. It indicates depression in the separated vortices, as intensive as it is inside of the boundary layer. This gives rise to strong and complex interactions between the plate and its wake, resulting in an aperiodic rocking motion. For computation of fluid forces it is therefore important to resolve with good accuracy not only the boundary layer, but also the vortical flow around the plate.

4 Conclusions and perspectives

A numerical method has been developed to solve the Navier–Stokes equations coupled with the equations which govern the free fall of a solid body. The two-dimensional Navier–Stokes equations in vorticity–stream

function formulation are discretized using a Fourier pseudo-spectral method with an adaptive second order Adams–Bashforth time stepping. The volume penalization method is used to impose the no-slip boundary condition on the boundary of the solid body. Solids of arbitrary shape can be modelled by simply changing the mask function in the penalization term, and it is also straightforward to generalize this approach to study flows past multiple solid bodies.

A numerical simulation of a tumbling plate at $Re = 1100$ has been compared with similar results in [1,6]. The agreement is adequate for a qualitative study. Numerical simulations at $Re = 10{,}100$ and 1000 have shown that decreasing Re has a stabilizing effect on the free fall dynamics, an observation which agrees with experimental results [12,13,5]. It is important to note that the number of grid points required to resolve the flow in the boundary layer is increasing as $N_x \times N_y \propto Re$. Hence, numerical simulations at Reynolds numbers up to a few thousands are feasible with the resolution of 102.4 grid points per chord length of the plate and a sufficiently large size of the periodic domain.

Perspectives for future work include a precise computation of the critical Reynolds number corresponding to the transition between steady descent and oscillatory motion, as well as its comparison with the critical Reynolds number for the flow past a fixed plate. Possibly the freely-falling plates can adapt their attitude in such a way as to delay the onset of oscillations, as it was recently suggested in [5] in the context of freely rising three-dimensional axisymmetric bodies. In this connection we are currently working to increase the order of accuracy of the numerical method, which would allow this kind of computations.

The extension of the model to three spatial dimensions is also planned. This will make possible a direct comparison with experiments, where the aspect ratio of the plate is finite.

Acknowledgements The authors thank the Deutsch-Französische Hochschule, project 'S-GRK-ED-04-05', for financial support. This work was performed using HPC resources from GENCI-IDRIS (Project 91664).

References

1. Andersen, A., Pesavento, U., Wang, Z.J.: Unsteady aerodynamics of fluttering and tumbling plates. J. Fluid Mech. **541**, 65–90 (2005a)
2. Andersen, A., Pesavento, U., Wang, Z.J.: Analysis of tranitions between fluttering, tumbling and steady descent of falling cards. J. Fluid Mech. **541**, 91–104 (2005b)
3. Angot, P., Bruneau, C.H., Fabrie, P.: A penalisation method to take into account obstacles in viscous flows. Numer. Math. **81**, 497–520 (1999)
4. Borisov, A.V., Kozlov, V.V., Mamaev, I.S.: On the fall of a heavy rigid body in an ideal fluid. Proc Steklov Inst Math **253**(SUPPL. 1), S24–S47 (2006)
5. Fernandes, P.C., Risso, F., Ern, P., Magnaudet, J.: Oscillatory motion and wake instability of freely rising axisymmetric bodies. J. Fluid Mech. **573**, 479–502 (2007)
6. Jin, C., Xu, K.: Numerical study of the unsteady aerodynamics of the freely falling plates. Commun. Comput. Phys. **3**(4), 834–851 (2008)
7. Kolomenskiy, D., Schneider, K.: A Fourier spectral method for the Navier-Stokes equations with volume penalization for moving solid obstacles. J. Comput. Phys. **228**, 5687–5709 (2009)
8. Maxwell, J.C.: On a particular case of the decent of a heavy body in a resisting medium. Camb. Dublin Math. J., **9**, 145–148 (1853); also Scientific Papers, **1**, 115–118 (Cambridge University, 1890)
9. Pesavento, U., Wang Z.J.: Falling paper: Navier-Stokes solutions, model of fluid forces, and center of mass elevation. Phys. Rev. Lett. **93**, 144501 (2004)
10. Schneider, K.: Numerical simulation of the transient flow behaviour in chemical reactors using a penalization method. Comput. Fluid. **34**, 1223–1238 (2005)
11. Schneider, K., Farge, M.: Numerical simulation of the transient flow behaviour in tube bundles using a volume penalization method. J. Fluids Struct. **20**, 555–566 (2005)
12. Smith, E.H.: Autorotating wings: an experimental investigation. J. Fluid Mech. **50**(3), 513–534 (1971)
13. Willmarth, W.W., Hawk, N.E., Harvey, R.L.: Steady and unsteady motions and wakes of freely falling disks. Phys. Fluids **7**, 197–208 (1964)